Intranuclear DNA density affects chromosome condensation in metazoans

Yuki Hara[a,b,*], Mari Iwabuchi[c], Keita Ohsumi[c], and Akatsuki Kimura[a,b]
[a]Cell Architecture Laboratory, Structural Biology Center, National Institute of Genetics, Yata 1111, Mishima, Shizuoka 411-8540, Japan; [b]Department of Genetics, School of Life Science, Graduate University for Advanced Studies (SOKENDAI), Yata 1111, Mishima, Shizuoka 411-8540, Japan; [c]Laboratory of Molecular Genetics, Division of Biological Science, Graduate School of Science, Nagoya University, Furo-cho, Chikusa-ku, Nagoya, Aichi 464-8602, Japan

ABSTRACT **Chromosome condensation is critical for accurate inheritance of genetic information. The degree of condensation, which is reflected in the size of the condensed chromosomes during mitosis, is not constant. It is differentially regulated in embryonic and somatic cells. In addition to the developmentally programmed regulation of chromosome condensation, there may be adaptive regulation based on spatial parameters such as genomic length or cell size. We propose that chromosome condensation is affected by a spatial parameter called the chromosome amount per nuclear space, or "intranuclear DNA density." Using *Caenorhabditis elegans* embryos, we show that condensed chromosome sizes vary during early embryogenesis. Of importance, changing DNA content to haploid or polyploid changes the condensed chromosome size, even at the same developmental stage. Condensed chromosome size correlates with interphase nuclear size. Finally, a reduction in nuclear size in a cell-free system from *Xenopus laevis* eggs resulted in reduced condensed chromosome sizes. These data support the hypothesis that intranuclear DNA density regulates chromosome condensation. This suggests an adaptive mode of chromosome condensation regulation in metazoans.**

Monitoring Editor
Kerry S. Bloom
University of North Carolina

Received: Jan 23, 2013
Revised: May 24, 2013
Accepted: Jun 7, 2013

INTRODUCTION

During cell division, DNA becomes highly compacted for segregation of genetic information into future daughter cells. Chromosome condensation is a crucial process because defective chromosome condensation can lead to segregation defects such as aneuploidy and cancer (Jallepalli and Lengauer, 2001; Nasmyth, 2002). The degree of condensation is actively regulated, as different condensed chromosome sizes are observed even in individual organisms possessing identical base-pair lengths of DNA. Condensed metaphase chromosomes become shorter and thicker as development progresses during the late embryonic phase of *Xenopus laevis* (Micheli *et al.*, 1993). This trend can be reproduced in a cell-free system from *X. laevis* egg (Kieserman and Heald, 2011). Similar observations have been reported in other species (Conklin, 1912; Frankhauser, 1934; Berardino, 1962; Belmont *et al.*, 1987). Therefore the sizes of condensed chromosomes are controlled by developmental stage–dependent regulation.

Several mechanisms mediate the developmentally programmed regulation of condensed chromosome size. The first mechanism involves condensin, a major regulator of chromosome condensation (Hirano and Mitchison, 1994; Hirano *et al.*, 1997). The ratio of condensin I and II changes between embryonic and somatic cells (Ono *et al.*, 2003), and this change is sufficient to reconstruct relatively long and short condensed chromosomes in a cell-free extract of *X. laevis* egg (Shintomi and Hirano, 2011). Similarly, two different developmental isoforms of the linker histone H1—embryonic H1M and somatic H1—may also define the size of embryonic and somatic chromosomes in *X. laevis* (Maresca *et al.*, 2005; Freedman and Heald, 2010). Density at the DNA replication origin may be involved in developmental control of condensed chromosome size. Because the position of the DNA replication origin can define the size of DNA loop structures (Buongiorno-Nardelli *et al.*, 1982; Courbet *et al.*, 2008) and the density of the origin decreases as development proceeds, it has

This article was published online ahead of print in MBoC in Press (http://www.molbiolcell.org/cgi/doi/10.1091/mbc.E13-01-0043) on June 19, 2013.

*Present address: Genome Biology Unit, European Molecular Biology Laboratory, Heidelberg 69117, Germany.

Address correspondence to: Akatsuki Kimura (akkimura@nig.ac.jp).

Abbreviations used: GFP, green fluorescent protein; GS, genome size; NR, nuclear radius; PR, packing ratio; RNAi, RNA-mediated interference; WGA, wheat germ agglutinin.

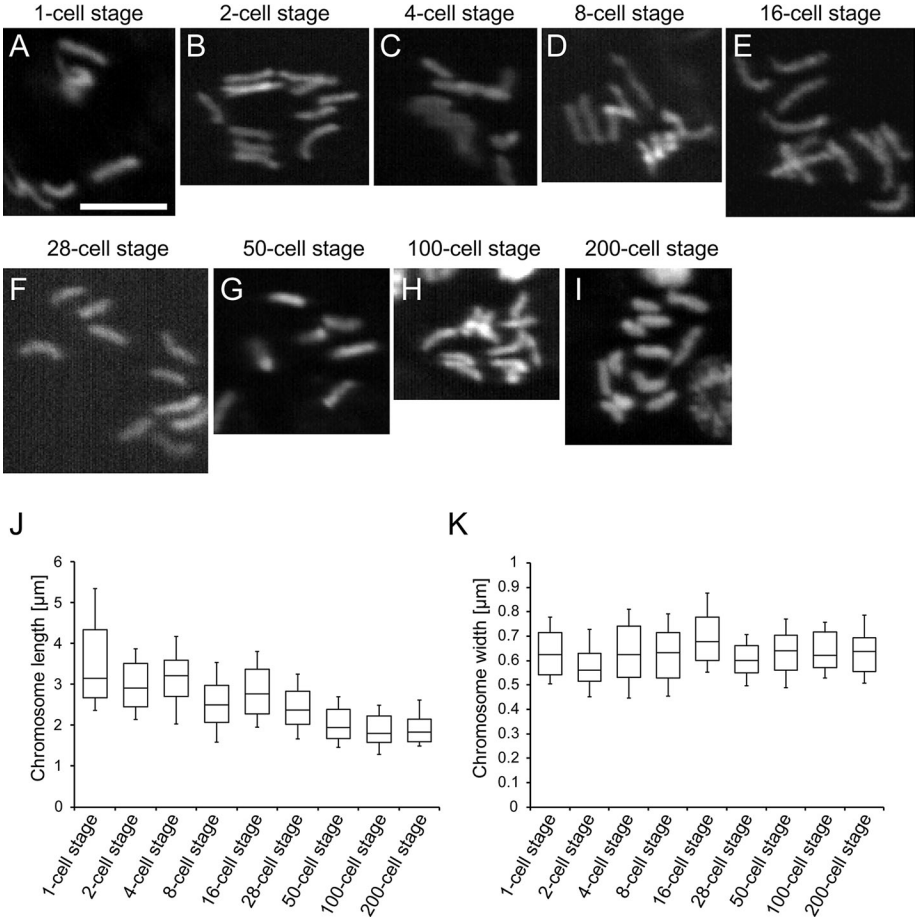

FIGURE 1: Individual condensed chromosome size is not constant during early embryogenesis. (A–I) Chromosomes in squashed embryos at each cell stage; bar = 5 μm. (J) The lengths and (K) widths of chromosomes at each cell stage are shown in the box plot. The middle line of each box is the median. The top and bottom lines are the third and first quartiles, respectively, and the whiskers indicate the 90th and 10th percentiles. The distributions of chromosome length and width in each cell stage are shown in histograms (Supplemental Figures S1 and S2).

been proposed that the change in origin density induces changes in condensed chromosome size during development (Micheli *et al.*, 1993; Pflumm, 2002).

In addition to the developmentally programmed regulation, chromosome condensation is likely controlled by adaptive mechanisms (Neurohr *et al.*, 2011). Here "adaptive" means that the degree of chromosome condensation is adjusted to the physical environment of the chromosome, even in cells of the same type and developmental stage. In *Saccharomyces cerevisiae*, an introduced extra-long chromosome is condensed to a higher degree to make the physical size of the introduced chromosome comparable to that of native chromosomes (Neurohr *et al.*, 2011). This adaptation is likely important to segregate daughter chromosomes completely over a limited distance of spindle elongation and may be regulated by a "midzone-based ruler" in which insufficient condensation is detected at the midzone during chromosome segregation and triggers more condensation.

Adaptive regulation may be appropriate for intact chromosomes in metazoans. In multicellular organisms, the size of cell varies within the organism, in particular during embryogenesis, and thus the adaptive regulation of chromosome condensation may take place (Kieserman and Heald, 2011; Ladouceur *et al.*, 2011). *Caenorhabditis elegans* embryogenesis is a good model in which to study the dependence of cellular processes in various spatial contexts, as transparent embryonic cells with various sizes of cell, nucleus, or spindle are observed (Carvalho *et al.*, 2009; Hara and Kimura, 2009, 2011; Greenan *et al.*, 2010; Ladouceur *et al.*, 2011). We identified variety in the extent and speed of spindle elongation in *C. elegans* embryogenesis (Hara and Kimura, 2009). Considering the possible connection between chromosome condensation and spindle elongation in *S. cerevisiae* (Neurohr *et al.*, 2011), we expected to see similar variety in condensed chromosome size during *C. elegans* embryogenesis.

RESULTS

Condensed chromosome length varies during *C. elegans* embryogenesis

To characterize the variation in condensed chromosome size, we observed separated chromosomes in *C. elegans* embryos at various cell stages. Squashes from acetic acid–fixed embryos allowed us to visualize 12 individual, rod-shaped mitotic chromosomes in a single cell of a *C. elegans* diploid hermaphrodite (Figure 1, A–I; Albertson and Thomson, 1982; Yoshida *et al.*, 1984). We measured samples in which the chromosomes were uniformly spread in what we define as prometaphase and metaphase chromosomes. We did not measure samples in which chromosomes segmented into two subgroups, as these represent anaphase or telophase. We measured the physical length and width of the condensed chromosomes, hereafter referred to as chromosome length and width, respectively (Figure 1, J and K, and Supplemental Figures S1 and S2). At different cell stages, chromosome lengths varied, as shown in the box plot (Figure 1J) and histograms (Supplemental Figure S1). The possible causes of this variability include 1) variable genomic lengths (e.g., chromosome III is 12.77 Mbp and chromosome V is 20.82 Mbp long; *C. elegans* Sequencing Consortium, 1998), 2) variability in cell cycle phase (i.e., prometaphase or metaphase), and 3) experimental variability. Note that the coefficient of variation (i.e., SD/mean) of the chromosome length was similar in all cell stages (Table 1), suggesting that our method was not biased toward a specific chromosome or cell cycle phase. Regardless of the variability, chromosome length clearly appeared to decrease as embryogenesis proceeded (Figure 1J). For example, chromosome length at the 2-cell stage is significantly larger than at the 100-cell stage ($p < 0.001$; mean value ± SE for 2-cell stage, 3.0 ± 0.1 [$n = 50$]; for 100-cell stage, 1.9 ± 0.04 [$n = 135$]). No apparent differences in chromosome width were noted (Figure 1K and Supplemental Figure S2). We do not have a good explanation for why the *C. elegans* chromosomes shorten but do not widen. In summary, our measurements indicated that the length, but not the width, of individual chromosomes decreases during *C. elegans* embryogenesis. The data indicate that the degree of chromosome condensation differs among cell stages.

			1-cell stage	2-cell stage	4-cell stage	8-cell stage	16-cell stage	28-cell stage	50-cell stage	100-cell stage	200-cell stage
Wild type	Chromosome length	Mean	3.6 (1.3)	3.0 (0.7)	3.2 (0.8)	2.6 (0.7)	2.8 (0.8)	2.4 (0.6)	2.0 (0.5)	1.9 (0.5)	1.9 (0.5)
		CV	36.0	23.9	26.2	28.7	26.7	25.2	25.6	25.2	24.2
		N	47	50	56	84	151	212	193	135	107
	Chromosome width	Mean	0.6 (0.1)	0.6 (0.1)	0.6 (0.1)	0.6 (0.1)	0.7 (0.1)	0.6 (0.1)	0.6 (0.1)	0.6 (0.1)	0.6 (0.1)
		CV	17.5	20.7	23.4	19.3	19.3	14.5	16.6	17.2	17.2
		N	47	44	58	82	100	204	153	117	107
mei-1 (RNAi) haploid	Chromosome length	Mean	3.0** (0.7)	3.4** (0.7)	3.9* (1.1)	3.3* (0.9)	3.0 (0.7)	3.0* (1.0)	2.7* (0.8)	2.4** (0.8)	N.D.
		CV	23.7	20.9	28.8	28.5	22.3	32.2	30.2	31.0	
		N	23	20	33	29	66	61	55	74	
	Chromosome width	Mean	0.7 (0.1)	0.7* (0.1)	0.7 (0.2)	0.6 (0.1)	0.6* (0.1)	0.6 (0.1)	0.6** (0.1)	0.6* (0.1)	N.D.
		CV	17.8	15.0	24.9	21.4	19.7	18.1	12.9	18.5	
		N	23	20	33	29	66	61	55	74	
klp-18 (RNAi) haploid	Chromosome length	Mean	3.4 (0.8)	3.8* (0.9)	3.5** (1.0)	3.3* (0.8)	3.2* (0.9)	2.8* (0.7)	2.7* (0.8)	2.1** (0.7)	N.D.
		CV	22.2	23.6	27.7	25.8	26.5	25.0	28.1	32.3	
		N	28	39	43	37	73	96	105	74	
	Chromosome width	Mean	0.7** (0.2)	0.7** (0.2)	0.7 (0.1)	0.6 (0.1)	0.6* (0.1)	0.6 (0.1)	0.6* (0.1)	0.5* (0.1)	N.D.
		CV	23.5	22.5	18.7	11.0	16.7	14.9	14.6	17.0	
		N	28	43	48	34	82	102	106	74	
klp-18 (RNAi) polyploid	Chromosome length	Mean	N.D.	2.3* (0.6)	2.7* (0.8)	2.8** (0.7)	2.1* (0.6)	2.3** (0.6)	1.7* (0.3)	1.3* (0.4)	N.D.
		CV		24.9	30.5	25.9	29.7	24.4	18.8	28.9	
		N		57	86	89	124	67	111	57	
	Chromosome width	Mean	N.D.	0.7* (0.2)	0.7 (0.1)	0.6 (0.1)	0.7 (0.1)	0.6 (0.1)	0.5* (0.1)	N.D.	N.D.
		CV		22.1	16.1	15.1	19.9	18.3	17.8		
		N		56	86	89	67	111	57		
ran-3 (RNAi)	Chromosome length	Mean	2.5* (0.9)	2.3* (0.7)	2.1* (0.6)	2.0* (0.6)	1.7* (0.5)	1.4* (0.4)	N.D.	N.D.	N.D.
		CV	35.6	30.6	30.6	28.1	27.2	24.5			
		N	40	50	68	77	100	64			
	Chromosome width	Mean	1.0* (0.1)	0.8* (0.1)	0.8* (0.1)	0.9* (0.2)	0.8* (0.1)	0.8* (0.1)	N.D.	N.D.	N.D.
		CV	15.3	17.5	15.9	18.3	15.9	10.5			
		N	40	59	63	62	80	52			
ima-3 (RNAi)	Chromosome length	Mean	3.1** (1.3)	2.4** (0.9)	2.5* (0.6)	2.3** (0.6)	2.1* (0.6)	2.2* (0.5)	1.8** (0.5)	1.5* (0.3)	N.D.
		CV	43.8	36.7	25.3	24.5	30.9	24.7	29.7	19.5	
		N	39	23	88	71	95	63	56	42	
	Chromosome width	Mean	0.7 (0.1)	0.6 (0.1)	0.7** (0.2)	0.7 (0.1)	0.6* (0.1)	0.6** (0.1)	0.6 (0.1)	0.5* (0.1)	N.D.
		CV	18.7	23.0	22.4	19.8	17.0	17.2	16.7	15.1	
		N	37	22	88	69	95	62	56	42	
C27D9.1 (RNAi)	Chromosome length	Mean	4.2 (0.8)	3.8* (1.1)	2.9 (0.9)	3.2* (0.8)	2.8 (0.7)	2.3 (0.6)	2.5* (0.8)	2.0** (0.6)	2.1 (0.5)
		CV	19.5	30.1	29.0	24.9	23.9	27.8	30.6	27.3	22.9
		N	10	67	27	110	163	61	81	96	28
	Chromosome width	Mean	0.8 (0.1)	0.7 (0.1)	0.6* (0.1)	0.6 (0.1)	0.6 (0.1)	0.6* (0.1)	0.6** (0.1)	0.5 (0.1)	0.6 (0.1)
		CV	12.5	18.4	17.9	17.4	13.5	12.2	13.6	13.7	13.1
		N	14	90	52	124	172	61	92	91	33

Mean length and width of the condensed chromosome (micrometers). SDs are shown in parentheses. CV, coefficient of variation; *N*, sample size examined; N.D., not determined. Asterisks indicate statistical differences from the wild type (*$p < 0.005$, ** $0.005 < p < 0.05$).

TABLE 1: Length and width of individual chromosomes in *C. elegans* embryos.

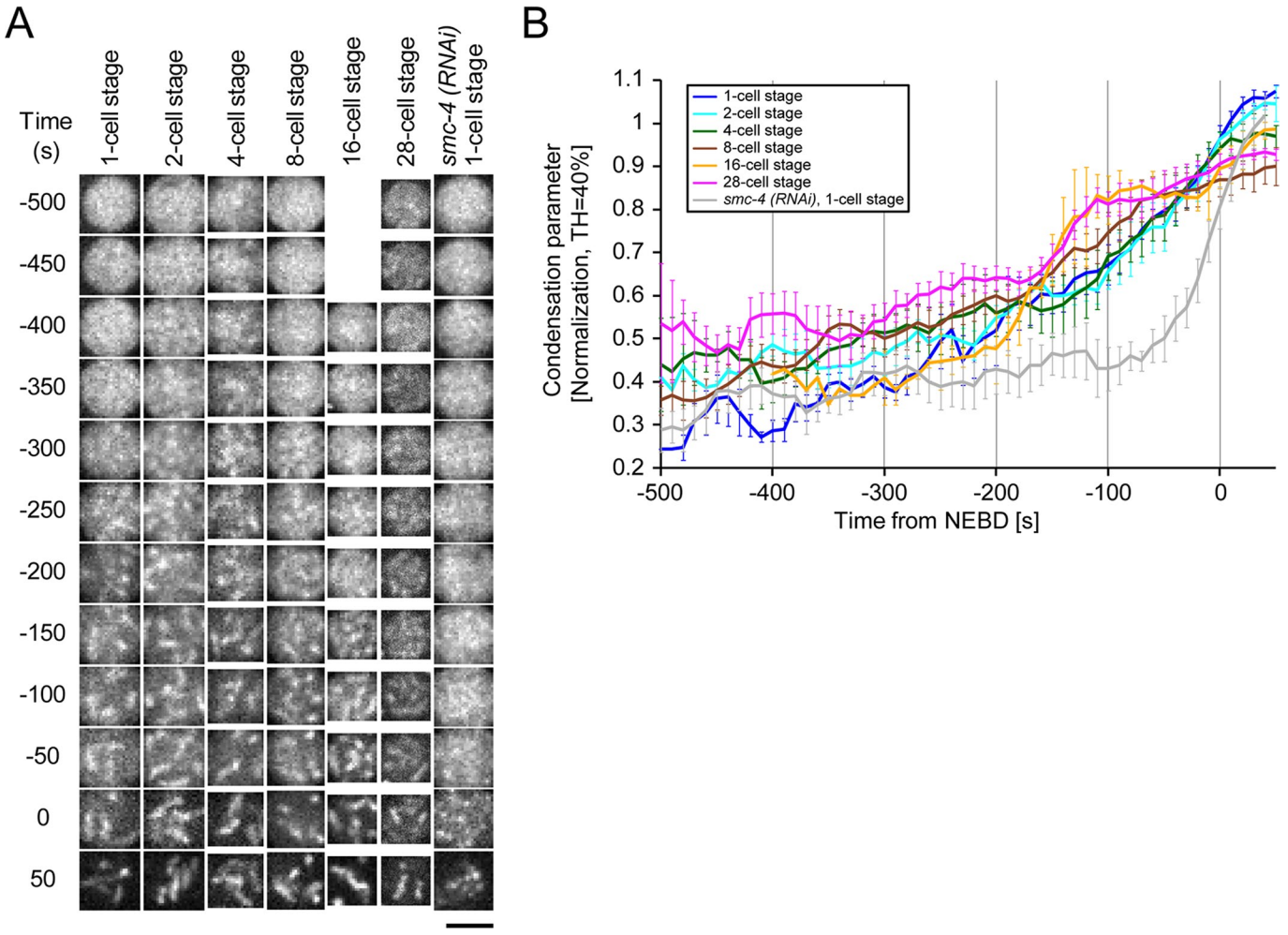

FIGURE 2: Dynamics of chromosome condensation in various cell stages. (A) Representative nuclear images at various cell stages of a control embryo and one-cell-stage *smc-4* (RNAi) embryo. Images are at 50-s intervals. Time corresponds to NEBD of 0. Bar, 5 μm. (B) Average of condensation parameter versus time. Colors indicate data from different cell stages of wild-type embryos (blue, 1-cell stage, male pronucleus, $n = 6$; light blue, 2-cell stage, $n = 5$; green, 4-cell stage, $n = 7$; brown, 8-cell stage, $n = 8$; yellow, 16-cell stage, $n = 2$; pink, 28-cell stage, $n = 8$) and one-cell-stage *smc-4* (RNAi) embryos (gray, $n = 5$). The average condensation parameter was calculated after aligning the sequences to NEBD. Error bars are SE. The sudden increase in the condensation parameter in *smc-4* (RNAi) around NEBD likely reflects the diffusion of free histones throughout the cytoplasm and might not reflect a change in chromosome condensation.

Chromosome condensation dynamics is similar during early embryogenesis

Possible explanations for the difference in condensed chromosome sizes include that 1) chromosome condensation is regulated by varying amounts of condensation regulators inside the cell (Maresca *et al.*, 2005; Maddox *et al.*, 2006; Shintomi and Hirano, 2011) and 2) the duration of chromosome condensation differs. Higher amounts of condensation regulators should lead to swifter condensation, and longer condensation time should lead to greater condensation. To examine whether the speed or the duration of chromosome condensation increases as embryogenesis proceeds, we compared the dynamics of chromosome condensation among various cell stages using an established method (Maddox *et al.*, 2006). The fluorescence intensity distribution of green fluorescent protein (GFP) fused with histone (GFP::histone) allows us to detect changes in chromosome condensation during mitosis. First, we conducted time-lapse imaging of GFP::histone during prophase until the onset of nuclear envelope breakdown (NEBD; Figure 2A). Using the histone distribution data, we quantified and compared chromosome condensation profiles in various cell stages (Figure 2B). In one-cell-stage embryos, the condensation score increases monotonically as chromosome condense, and the difference in condensation kinetics between wild-type and condensin-perturbed embryos (*smc-4*/SMC4; RNA-mediated interference [RNAi]) was clear (Maddox *et al.*, 2006; Figure 2B). When we compared the kinetics among cell stages, the overall profile of chromosome condensation was similar (Figure 2B). Thus the speed and duration of chromosome condensation were similar among different cell stages during early embryogenesis. These data suggest that a drastic change in condensation dynamics (such as changes in major chromosome condensation regulators during the stages of interest) is unlikely. Because the condensation kinetics is similar among the different cell stages but the final condensed chromosomes differ in size, we hypothesized that precondensation differences influence the degree of condensation.

Ploidy changes the size of the condensed chromosomes

Because nuclear size changes during embryogenesis, chromosome density in the interphase nucleus varies and may affect the initial

state of the chromosomes before condensation. The involvement of chromosome density in chromosome condensation is consistent with our observation that condensed chromosomes from one-cell-stage embryos are significantly longer than in two-cell-stage embryos (Figure 1J; $p < 0.05$). The one-cell-stage embryo has two pronuclei and contains a haploid genome, whereas the nuclei at the two-cell stage contain diploid genomes. Because nuclear size at the two-cell stage is almost comparable to that of pronuclei at the one-cell stage, chromosome density inside the nucleus differs between stages and correlates negatively with chromosome length.

To manipulate chromosome density in the nucleus, we generated haploid embryos by RNAi knockdown of the *klp-18*/kinesin 12 gene. This RNAi embryo occasionally extrudes all of the oocyte genome into polar bodies due to meiotic division failure (Supplemental Figure S3; Segbert *et al.*, 2003). This causes the *klp-18* (RNAi) embryo to possess chromosomes only from the sperm, yielding a haploid genome (Hara and Kimura, 2013). From the *klp-18* (RNAi) embryos, we selected haploid embryos by confirming the absence of the female pronucleus or six chromosomes per nucleus (Supplemental Figures S3 and S4). These are called "*klp-18* (RNAi) haploid" embryos. The chromosome lengths of *klp-18* (RNAi) haploid embryos were significantly larger than those at the corresponding cell stage in the wild type (Figure 3 and Table 1).

klp-18 is unlikely to be directly involved in chromosome condensation. Some *klp-18* (RNAi) embryos retained the majority or entire maternal compliment of DNA in the embryo, yielding an excess of DNA (polyploid; Segbert *et al.*, 2003; Hara and Kimura, 2013). We observed chromosomes of *klp-18* (RNAi) polyploid embryos by selecting embryos with excess DNA or >12 chromosomes per nucleus (Supplemental Figure S4). The chromosomes of *klp-18* (RNAi) polyploid embryos were shorter than those of *klp-18* (RNAi) haploid and those of wild-type diploid embryos (Figures 3 and Table 1). This observation indicated that the change in chromosome length is negatively correlated with chromosome number in the embryos. In addition, one-cell (pronuclear)–stage *klp-18* (RNAi) and wild-type embryos and two-cell-stage *klp-18* (RNAi) haploid embryos, all of which possess the same DNA content per (pro)nucleus, had condensed chromosomes of almost the same size (Table 1). Finally, we obtained haploid embryos by *mei-1*/katanin (RNAi) (Mains *et al.*, 1990; Hara and Kimura, 2013) and observed longer chromosomes (Figure 3 and Table 1). On the basis of these data, we concluded that the change in chromosome number caused a change in the length of the condensed chromosome. Thus the degree of chromosome condensation is not solely defined by developmental stage but might depend on spatial context.

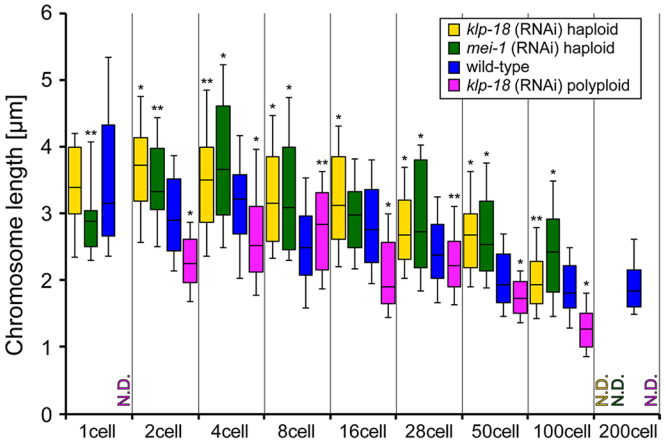

FIGURE 3: Reduced or increased DNA content leads to increased or reduced condensed chromosome size, respectively. The lengths of condensed chromosomes at each cell stage are shown in the box plot. Data for wild-type (blue), *klp-18* (RNAi) haploid (yellow), *klp-18* (RNAi) polyploid (pink), and *mei-1* (RNAi) haploid (green) embryos. Chromosome lengths at almost all stages, except for the one-cell stage (haploid per pronucleus only at the one-cell stage) in *klp-18* (RNAi) haploid or *mei-1* (RNAi) haploid embryos, were significantly larger than those of wild-type embryos (Student's *t* test). *$p < 0.005$; **$0.005 < p < 0.05$. The chromosome lengths in *klp-18* (RNAi) polyploid embryos were significantly smaller than those of wild-type embryos at each cell stage. Note that the pronuclei contained a haploid genome in wild-type and *klp-18* or *mei-1* (RNAi) embryos at the one-cell stage. The middle line of each box is the median. The top and bottom lines are the third and first quartiles, respectively, and the whiskers indicate 90th and 10th percentiles. N.D., not determined. Mean length, SD, and sample size are shown in Table 1.

The changes in chromosome length induced by changing the chromosome number should be independent of the midzone-based ruler mechanism proposed in *S. cerevisiae* (Neurohr *et al.*, 2011). First, we are observing chromosomes of prometaphase and metaphase, and the change should take place before chromosome segregation at anaphase. Second, with this mechanism, the longer chromosome can be explained by faster chromosome separation at anaphase or larger cell size (Ladouceur *et al.*, 2011). This was not the case for *klp-18* (RNAi) haploid embryos. The speed of chromosome separation (measured as the speed of spindle elongation) in *klp-18* (RNAi) haploid embryos was not faster than the controls at corresponding cell stages (Supplemental Table S1). The cell size in *klp-18* (RNAi) haploid embryos was comparable to that in wild-type embryos (cell length in the one-cell stage of wild type, mean ± SE, 43.1 ± 0.3 μm [$n = 26$]; in the one-cell stage of *klp-18* (RNAi) haploid, 42.7 ± 0.9 μm [$n = 12$]). Third, the midzone-ruler mechanism predicts higher chromosome compaction with shorter spindles. This was not the case in our previous observation, as the short spindle in *spd-2*/Cep192 (RNAi) or *tpxl-1*/TPX2 (RNAi) did not affect chromatin condensation (Hara and Kimura, 2013). Instead of the midzone-based ruler mechanism, we propose that reduced DNA density inside the nucleus increased the size of the condensed chromosomes. The nuclear diameters in the *klp-18* (RNAi) haploid embryo were similar to those in the wild-type embryo (Supplemental Figure S3 and Table 2). A spatial parameter of intranuclear DNA density may affect the degree of chromosome condensation.

The ratio of DNA amount to nuclear size is correlated with chromosome size

To test our idea that intranuclear DNA density affects the degree of chromosome condensation, we further investigated the relationship between DNA density and chromosome condensation in the *C. elegans* embryo. First, we evaluated the quantitative relationship between intranuclear DNA density and condensed chromosome size during wild-type embryogenesis. As embryogenesis proceeds, the size of the nucleus decreases (Hara and Kimura, 2009; Figure 4A and Table 2), increasing the intranuclear DNA density. We plotted the relative ratio of the DNA amount to the nuclear size against the mean chromosome length in each cell stage (Figure 4B) for wild-type (including pronuclear stage) and *klp-18* or *mei-1* (RNAi) haploid nuclei. We did not include data from *klp-18* (RNAi) polyploid embryos because their exact ploidy could not be determined (Hara and Kimura, 2013). The relative ratio was calculated by dividing the genome length per (pro)nucleus (Mbp) by nuclear volume. The regression line fitted to the wild-type plot showed that the chromosome length correlated well with the relative DNA ratio; the line also explains the data from the haploid nucleus.

		1-cell stage	2-cell stage	4-cell stage	8-cell stage	16-cell stage	28-cell stage	50-cell stage	100-cell stage	200-cell stage
Wild type	Mean	8.8 (0.4)	9.1 (0.5)	8.0 (0.6)	7.1 (0.8)	6.2 (0.5)	5.4 (0.6)	3.8 (0.3)	3.3 (0.4)	3.1 (0.3)
	N	24	42	47	49	60	45	28	42	8
mei-1 (RNAi) haploid	Mean	8.6 (0.5)	8.6** (0.7)	7.6** (0.6)	6.6** (0.7)	5.4* (0.5)	4.1* (0.5)	N.D.	N.D.	N.D.
	N	7	12	13	16	17	26			
klp-18 (RNAi) haploid	Mean	9.2** (0.2)	9.2 (0.5)	7.9 (0.6)	6.9 (0.7)	6.4** (0.3)	5.4 (0.3)	4.3** (0.6)	N.D.	N.D.
	N	8	17	13	18	7	9	15		
klp-18 (RNAi) polyploid	Mean	N.D.	9.7** (0.5)	8.7 (0.8)	7.6 (0.8)	6.0 (0.7)	5.2 (0.5)	N.D.	N.D.	N.D.
	N		8	9	10	17	9			
ran-3 (RNAi)	Mean	5.4* (0.4)	6.3* (0.3)	6.1* (0.6)	5.3* (0.8)	5.2* (0.5)	4.6* (0.7)	N.D.	N.D.	N.D.
	N	7	6	17	11	26	18			
ima-3 (RNAi)	Mean	8.0** (0.7)	7.9* (0.6)	6.8* (0.6)	5.7* (0.9)	4.8* (0.6)	3.8* (0.7)	N.D.	N.D.	N.D.
	N	8	11	10	11	14	8			
C27D9.1 (RNAi)	Mean	9.8* (0.9)	9.8* (0.5)	8.6* (0.5)	7.9* (0.6)	7.0* (0.6)	5.3 (0.6)	4.3* (0.5)	3.6** (0.3)	3.5 (0.6)
	N	22	13	16	16	23	44	30	14	14

Mean nuclear diameter (micrometers). Diameter was measured just before nuclear envelope breakdown. Male and female pronuclei were measured in 1-cell wild-type and *ran-3, ima-3, C27D9.1* (RNAi) embryos. Only male pronucleus was measured in *klp-18* and *mei-1*(RNAi) haploid embryos. SDs are shown in parentheses. *N*, sample size; N.D., not determined. Asterisks indicate statistical differences from the wild type (*$p < 0.005$, **$0.005 < p < 0.05$).

TABLE 2: Diameter of the prophase nucleus in *C. elegans* embryos.

Next we attempted to manipulate nuclear size by knocking down genes. We knocked down *ran-3*/RCC1, *npp-13*/Nup93, *lmn-1*/Lamin, *emr-1*/Emerin;*lem-2*/MAN1, *ima-3*/Importin α3, and *arf-1*/ARF by RNAi because knockdown of each gene reduces nuclear size in one-cell-stage embryos (Poteryaev *et al.*, 2005; Sonnichsen *et al.*, 2005; Meyerzon *et al.*, 2009). RNAi of *ran-3* or *ima-3* caused a consistent reduction in nuclear size during embryogenesis at the 1- to 16-cell stage (Figure 4C and Table 2). RNAi knockdown of the other candidate genes revealed little effects on nuclear size after the two-cell stage (Supplemental Figure S5 and Supplemental Table S2). In *ran-3* or *ima-3* (RNAi) embryos, the individual chromosome length at all cell stages significantly decreased in comparison to the wild type (Figure 4D and Table 1). In addition, we examined the larger nuclei in *C27D9.1* (RNAi) embryos, which have larger cells (Figure 4C and Table 2; Hara and Kimura, 2009). The chromosomes in *C27D9.1* (RNAi) embryos were longer than in the wild type (Figure 4D and Table 1).

When we plot the data from *ran-3, ima-3*, and *C27D9.1* (RNAi) chromosome length versus DNA density, we find an overall trend similar to the data from wild-type and *klp-18* or *mei-1* (RNAi) haploid embryos and near the regression line (Figure 4B). In summary, changing the DNA ratio by changing nuclear size during embryogenesis or RNAi treatment caused chromosome length to change, supporting the hypothesis that intranuclear DNA density affects the degree of chromosome condensation.

Reduced nuclear size induces chromosome size reduction in a cell-free system from *X. laevis* eggs

To obtain completely independent experimental support for the idea that intranuclear DNA density affects the degree of chromosome condensation and to evaluate the generality of the idea, we tested our hypothesis using a cell-free system from *X. laevis* eggs. In this system, functional nuclei can be reconstituted by incubating sperm nuclei in *X. laevis* egg extract at the interphase (Figure 5A). Furthermore, the nuclei can be transformed to condensed chromosomes by inducing the cell-cycle transition of the extract to M phase (Hirano and Mitchison, 1994; Desai *et al.*, 1997). We could reduce the nuclear size in this system by inhibiting nuclear growth with antibody against lamin LIII protein, which is a primary component of the nuclear lamina in *X. laevis* oocytes and early embryonic cells (Lourim *et al.*, 1996), or by adding wheat germ agglutinin (WGA), which blocks nuclear pores by binding to nucleoporins that contain *N*-acetylglucosamine residues (Finlay *et al.*, 1991; D'Angelo *et al.*, 2006). We preincubated sperm nuclei in the interphase egg extracts to allow nuclear formation and added the antibody or WGA to the extracts to suppress nuclear growth. Although complete inhibition of nuclear import without preincubation impairs DNA replication and nuclear envelope assembly (Cox, 1992; Hachet *et al.*, 2004), our experimental conditions allowed nuclear envelope formation and complete DNA replication (D'Angelo *et al.*, 2006; Supplemental Figure S6). We obtained functional small nuclei by adding anti–lamin LIII antibodies or WGA to the cytoplasmic extract (Figure 5B and Table 3).

Extracts containing these reconstructed nuclei were transformed to condensed chromosomes by adding nondestructible cyclin B protein to the extracts (Figure 5C). The chromosomes in all three experiments appeared to consist of a pair of sister chromatids (Figure 5C). The chromosomes in anti–lamin LIII antibody– or WGA-treated extract were normal in overall appearance but were smaller

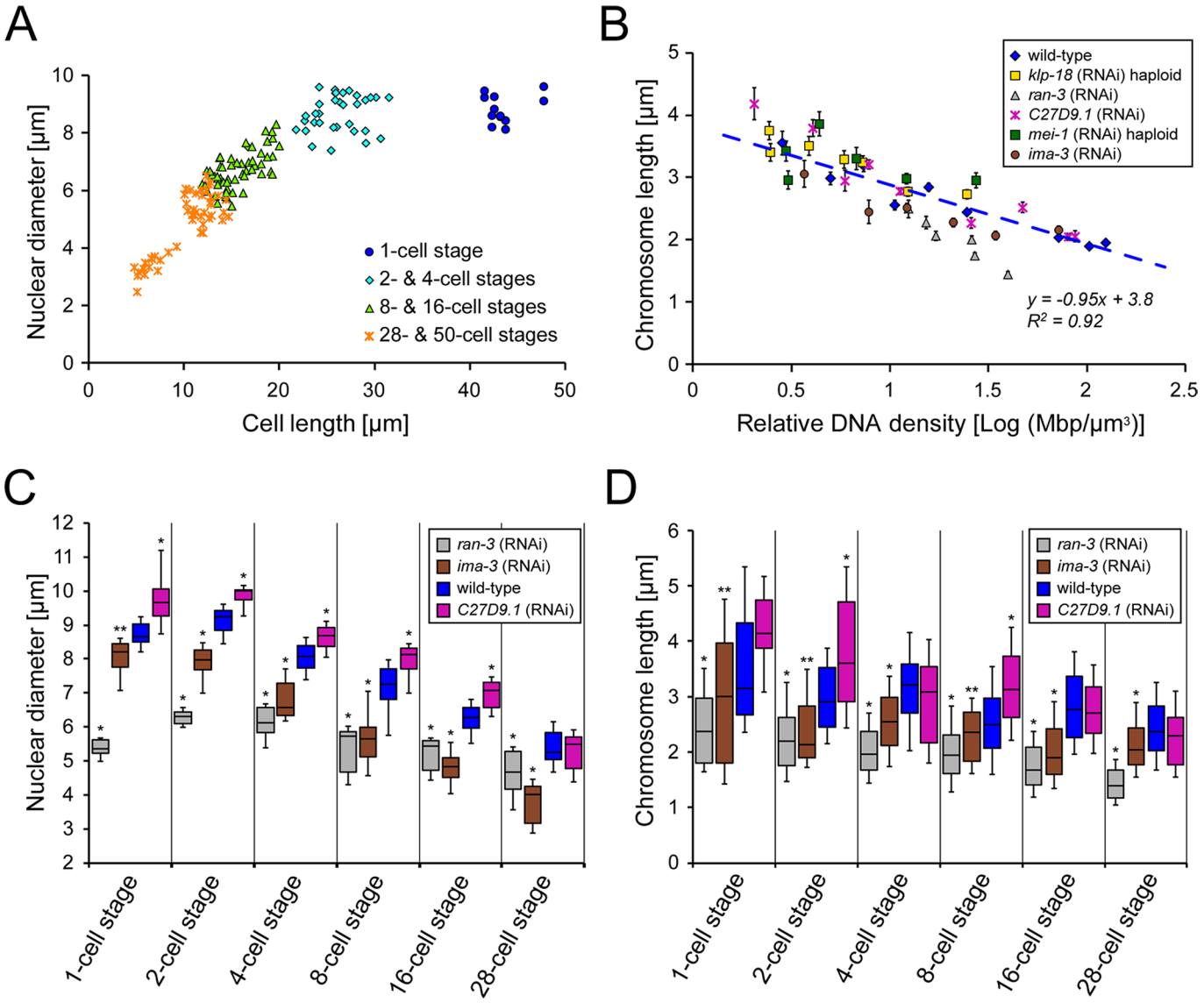

FIGURE 4: Nucleus size affects condensed chromosome size. (A) Relationship between measured nuclear diameter and cell length at various cell stages of wild-type embryos. Different shapes and colors represent each cell stage: blue circle, 1-cell stage; light blue diamond, 2- and 4-cell stages; green triangle, 8- and 16-cell stages; orange cross, 28- and 50-cell stages. (B) Mean chromosome length at each cell stage was plotted as function of the calculated relative DNA density. Data for wild-type (blue diamond), *klp*-18 (RNAi) haploid (yellow rectangle), *mei-1* (RNAi) haploid (green rectangle), *ran-3* (gray triangle), *ima-3* (brown circle), and *C27D9.1* (RNAi) embryos (pink cross). We do not include data from *klp-18* (RNAi) polyploid embryo because the exact ploidy of the embryos could not be determined. The regression line for the wild-type data is shown. Error bars are SE. (C) Individual nuclear diameters for wild-type (blue), *ran-3* (gray), *ima-3* (brown), and *C27D9.1* (RNAi) embryos (pink) at each cell stage are shown in the box plot. The nuclear diameters in each RNAi embryo in all cell stages were significantly different from those of wild-type embryos (Student's *t* test). (D) Chromosome length at most cell stages in *ran-3, ima-3, C27D9.1* (RNAi) embryos significantly differed from those of wild-type embryos (Student's *t* test). *$p < 0.005$; **$0.005 < p < 0.05$. The middle line of each box is the median. The top and bottom lines are the third and first quartiles, respectively, and the whiskers indicate the 90th and 10th percentiles. Mean chromosome length, nuclear diameter, SD, and sample size are shown in Tables 1 and 2.

and thicker than those in the control extract (Figure 5, D and E and Table 3). Thus intranuclear DNA density affects the degree of chromosome condensation.

Estimation of the linear packing ratio suggests general trends between packing ratio and intranuclear DNA density

To compare chromosome condensation between species, we used linear packing ratio to represent chromosome condensation. Linear packing ratio is the DNA length (0.34 nm/base pair) divided by the length into which it is packaged. The average DNA length per chromosome in *C. elegans* and *X. laevis* is ~5700 µm (17 Mbp = 100 Mbp/6 chromosomes) and 59,000 µm (170 Mbp = 3100 Mbp/18 chromosomes), respectively. Thus we assumed an allometric relationship between the packing ratio (PR), genome size (GS [Mbp]), and nuclear radius (NR [µm]) as $PR = GS^{\alpha} \times NR^{\beta} \times C$, where α, β, and C are constants. We calculated these constants by the least-squares

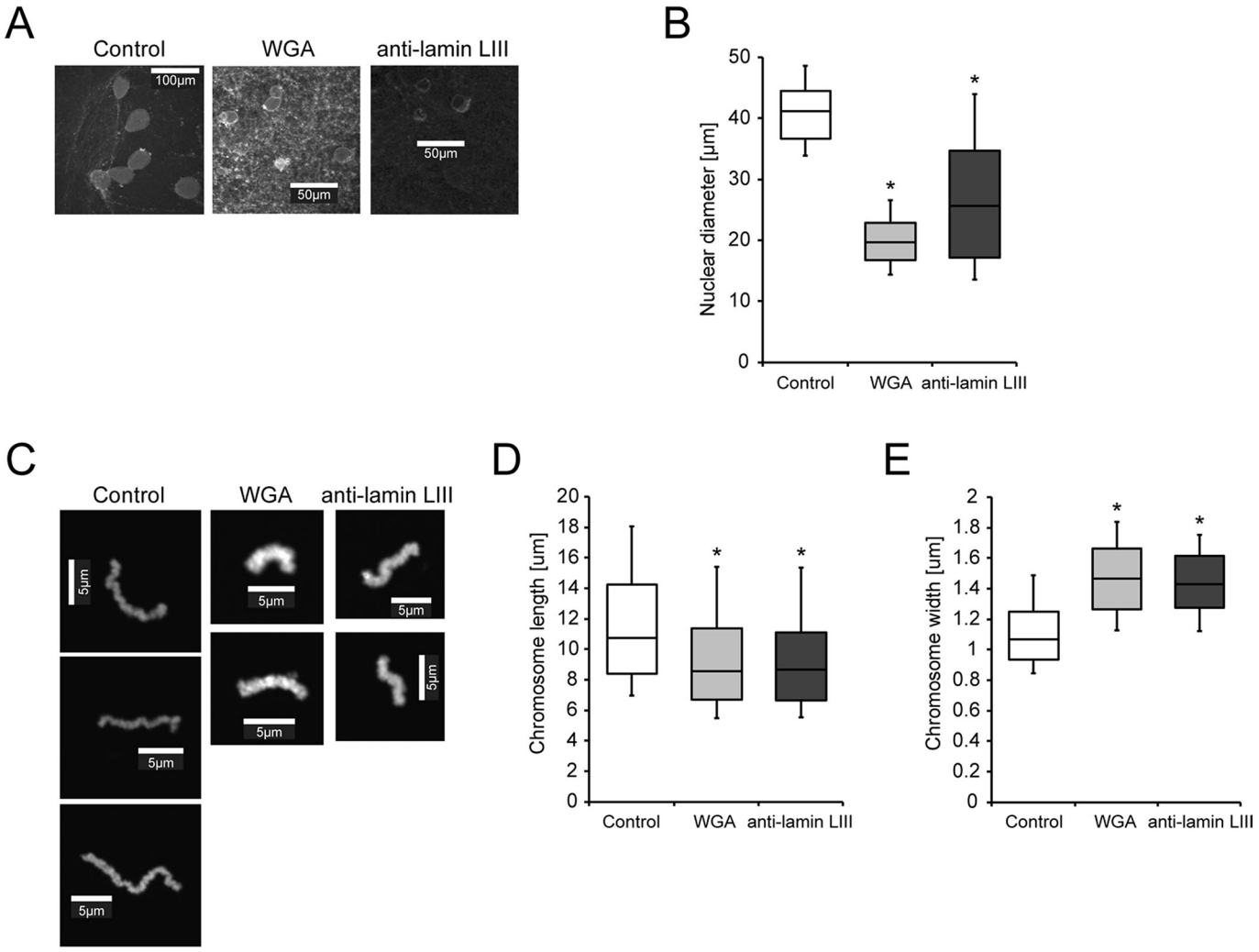

FIGURE 5: Chromosome sizes reconstructed in vitro using *X. laevis* egg extracts. (A) Examples of nuclei reconstructed from control extracts, with WGA, or with anti–lamin LIII antibody. (B) Quantified nuclear diameters in the extracts for control, WGA, and anti-lamin LIII antibody. (C) Representative chromosomes reconstituted with the extracts after nuclear formation. (D, E) Length (D) and width (E) of the reconstituted chromosomes. The middle line of each box is the median. The top and bottom lines are the third and first quartiles, respectively, and the whiskers indicate the 90th and 10th percentiles. Mean chromosome length, chromosome width, nuclear diameter, SD, and sample size are shown in Table 3. *$p < 0.005$.

method. We used literature data for *X. laevis* (Supplemental Table S3), as well as the *C. elegans* and *X. laevis* data obtained in this study. We calculated α and β as 0.41 and −0.35, respectively. Because α and β had similar absolute values, we simplified the allometric relationship as $PR = (GS/NR)^{\gamma} \times C'$. We recalculated the value of γ and C' and obtained a fitting equation, $PR = 440(GS/NR)^{0.41}$ (Figure 6). Of interest, not only the data used for the fitting but also some data measured in *Drosophila*, *Xenopus tropicalis*, mouse, and human cells (Supplemental Table S3) were plotted near the line (Supplemental Figure S7). Note that other data from humans, rats, and mice were plotted far from the fitting curve (Supplemental Figure S7). It will be an interesting future project to compare the sizes of condensed chromosomes from different species under a controlled experimental condition. Although some data from mammalian cells did not fit, our observation that plots from different organisms aligned to a common line implies that the ratio between genome size and nuclear size might be a universal parameter of chromosome condensation.

DISCUSSION

About 100 years ago, Conklin (1912) proposed that the size of a chromosome depends on the size of the nucleus, based on cytological observation. The role of nuclear size in chromosome condensation, however, has been largely overlooked. In this study, we propose that intranuclear DNA density is one of the determinants of mitotic chromosome condensation. In this study, we demonstrated a correlation between nuclear size and chromosome condensation in *C. elegans* 1) during normal embryogenesis, 2) when nuclear size was reduced by knocking down *ran-3*/RCC1 and *ima-3*/Importin α3, and 3) when nuclear size was increased by knocking down *C27D9.1*. In addition, the smaller nucleus reconstituted in *Xenopus* egg cell-free extract resulted in shorter chromosomes. It has been proposed that the size of the nucleus does not directly affect the length of condensed chromosomes in a cell-free system of *Xenopus* egg (Kieserman and Heald, 2011). The proposal is superficially inconsistent with our argument. Our data and the previous report, however, are quantitatively consistent. Kieserman and Heald (2011)

		Control	WGA	Anti–lamin LIII
Chromosome length	Mean	11.8 (4.6)	9.8* (4.4)	9.7* (4.3)
	CV	1.1	1.6	2.3
	N	440	280	188
Chromosome width	Mean	1.1 (0.3)	1.5* (0.3)	1.4* (0.3)
	CV	0.1	0.1	0.1
	N	437	280	188
Nuclear diameter	Mean	40.8 (6.8)	20.5* (5.6)	27.1* (11.6)
	CV	4.5	3.7	7.6
	N	152	150	152

Mean length and width of the condensed chromosome and nuclear diameters (micrometers). Diameter was measured in interphase nuclei after incubation for 120 min. SDs are shown in parentheses. CV, coefficient of variation; *N*, sample size examined. Asterisks indicate statistical differences from the control (*$p < 0.005$).

TABLE 3: Length and width of individual chromosomes and diameter of nuclei in *X. laevis* cell-free system.

demonstrated that the lengths of condensed chromosomes reconstituted from *X. laevis* extract and *X. tropicalis* extract were comparable, although the sizes of the nuclei before induction of chromosome condensation were significantly different. Here the expected size difference of the nuclei is ~1.5-fold in radius, based on a previous report from the same group (Levy and Heald, 2010). In our experiment using *X. laevis* extract, the radius difference between normal and small nuclei was about twofold. Under this condition, the length difference was statistically significant but only ~1.3-fold. Our measurement suggested that, for us to see a significant length change in condensed chromosomes, the nuclear radius should differ dramatically. Our measurement in *C. elegans* supports this notion. In comparison between 2- and 16-cell-stage wild-type embryos, the difference in nuclear radius was significant ($p < 0.01$) and 1.5-fold, whereas the difference in condensed chromosome size was not significant. In contrast, between cell stages in which the difference in nuclear radius is greater than twofold, the condensed chromosome length was always significantly different ($p < 0.01$). Therefore our measurements and the previous measurements (Kieserman and Heald, 2011) are quantitatively consistent.

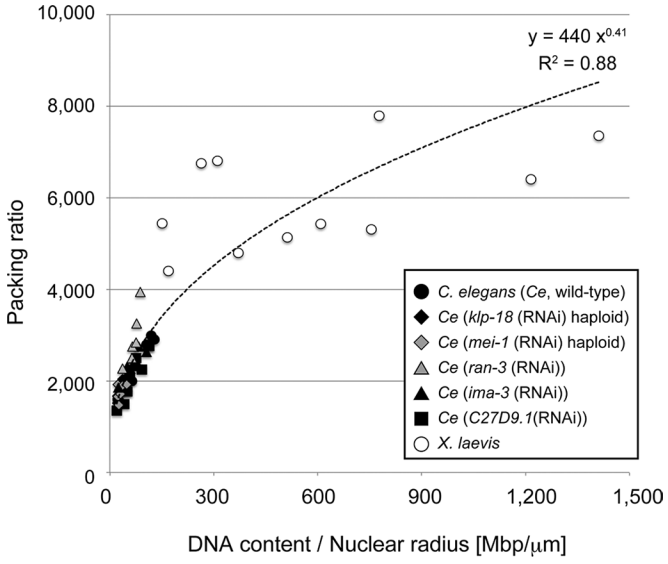

FIGURE 6: Curve fit of the estimated packing ratio vs. intranuclear DNA density. Linear packing ratio was plotted vs. intranuclear DNA density, which was calculated by dividing DNA content (Mbp) by the nuclear radius (μm). Data are summarized in Supplemental Table S3. The plot was fitted to the exponential curve with the least-squares method. Black circle, *C. elegans* wild type (diploid); black diamond, *C. elegans klp-18* (RNAi) haploid; gray diamond, *C. elegans mei-1* (RNAi) haploid; gray triangle, *C. elegans ran-3* (RNAi); black triangle, *C. elegans ima-3* (RNAi); black square, *C. elegans C27D9.1* (RNAi); white circle, *X. laevis*.

We also demonstrated a correlation between chromosome amount (ploidy) and chromosome condensation in *C. elegans*. In wild-type embryos, chromosomes from one-cell-stage pronuclei (haploid) were longer than those from two-cell-stage nuclei (diploid). Longer chromosomes were observed in haploid embryos induced by knocking down *klp-18*/kinesin 12 or *mei-1*/katanin, whereas shorter chromosomes were observed in *klp-18* (RNAi) polyploid embryos. The correlation is consistent with previous studies in other species. Kieserman and Heald (2011) demonstrated that chromosomes from *X. tropicalis* sperm nuclei are longer than those from *X. laevis* sperm nuclei when incubated in the same extracts. *X. tropicalis* has a smaller genome, and the sizes of the reconstructed nuclei are similar (Levy and Heald, 2010). In the newt *Triturus palmatus*, the chromosomes of haploid blastulae are larger than those of diploid blastulae (Frankhauser, 1934). (In this study, nuclear size in the haploid *T. palmatus* blastulae was not measured.) In *Rana pipiens*, although the chromosome size in haploid embryos at stage 25 tail is comparable to that in diploid embryos (Berardino, 1962), the size of the nucleus is reduced in haploid embryos (Briggs, 1949). The aforementioned observations support our hypothesis that intranuclear density affects the length of compacted chromosomes.

How can the ratio of DNA amount to nuclear size affect the size of mitotic chromosomes? One possible scenario involves the formation of DNA loops. DNA loop formation was proposed to mediate the control of chromosome condensation by varying density of the replication origin (Pflumm, 2002). Because the replication origin is believed to be a bundle of DNA loops, the number of DNA loops is expected to decrease as the number of replication origins decreases, producing shorter condensed chromosomes. In fact, DNA loop size increases as development proceeds during *Xenopus* embryogenesis (Buongiorno-Nardelli *et al.*, 1982; Courbet *et al.*, 2008). The change in transcriptional status during development may also change DNA loop formation (Seydoux and Dunn, 1997; Cremer and Cremer, 2001). We believe that we can apply the concept of DNA loops defining the size of condensed chromosomes to the effect of intranuclear DNA density. For example, if we assume that the anchorage structures for DNA loop formation reside on the nuclear envelope with constant density, a large nucleus or fewer chromosomes should result in many DNA loops per chromosome and thus longer condensed chromosomes. In fact, the nuclear lamina and nuclear pore complex, which appear on the inner nuclear envelope, anchor DNA loops (Cremer and Cremer, 2001; Ishii *et al.*, 2002). Another possibility involves macromolecular crowding. When mitotic rodent fibroblasts are incubated in buffer containing an inert volume–occupying macromolecule, the sizes of the condensed chromosomes are shorter than those from cells incubated in buffer alone (Hancock, 2012). Because the DNA/chromosome itself is a macromolecule, the effect of intranuclear DNA density on

chromosome condensation may be mediated through general changes in macromolecular crowding.

Intranuclear density-dependent chromosome condensation relies on spatial parameters and is not developmentally programmed; the mechanism can be described as adaptive regulation of chromosome condensation. Adaptive regulation of chromosome condensation has been demonstrated in *S. cerevisiae*, where engineered long chromosome results in higher-order compaction at anaphase (Neurohr *et al.*, 2011). This adaptive regulation ensures that the resultant mitotic chromosome is not too long, so that chromosome segregation proceeds faithfully with a limited distance for spindle elongation (Neurohr *et al.*, 2011). The authors proposed that the midzone of the mitotic spindle at anaphase works as a ruler to measure the length of the mitotic chromosome and induce adaptive hypercondensation (Neurohr *et al.*, 2011). Thus chromosome size may be regulated by other factors, such as the environment inside the cell at other cell cycle stages (Ladouceur *et al.*, 2011). In this study, we observed changes in chromosome size before spindle formation; thus the regulation must be independent of the midzone-ruler mechanism. We were able to demonstrate intranuclear DNA density before nuclear envelope breakdown serves as a spatial constraint for setting mitotic chromosome size.

The biological significance of the intranuclear DNA density-dependent control of chromosome condensation is unclear. Adaptive chromosome condensation can be significant, as it depends on intranuclear density, and optimization requires a trade-off between chromosome compaction in mitotic phase and DNA transactions in interphase. Chromosome compaction is a crucial process, since defective compaction results in abnormal segregation (Hudson *et al.*, 2003; Ono *et al.*, 2003). In contrast, after cell division, the condensed chromosomes become decondensed and reconstitute the nucleus. This decondensation is believed to be important in allowing various transacting factors to bind DNA and activate transcription and replication. Such control may be particularly evident during embryogenesis, since the travel distance of a chromosome in segregation differs dramatically, depending on cell size (Hara and Kimura, 2009). When a chromosome segregates over a short distance in smaller cells, the chromosome must condense extensively to ensure complete condensation; this is less of a requirement in larger cells (Levy and Heald, 2012). Because nuclear size depends on the cell size (Goehring and Hyman, 2012), intranuclear DNA density-dependent adaptive chromosome condensation may be a mechanism to optimize the degree of chromosome condensation in response to cell size.

MATERIALS AND METHODS

C. elegans strains and RNAi procedure

To visualize individual chromosomes and the cell nucleus, we used wild-type *C. elegans* N2 and RNAi-treated N2 worms, strain CAL0061 expressing GFP–γ-tubulin (*tbg-1*), GFP–histone H2B (*his-11*), and GFP–PHPLCdelta-1, and strain TH32 (Hara and Kimura, 2009). For RNAi, double-strand RNA was prepared and injected as described previously (Kimura and Onami, 2005). The templates for *smc-4, klp-18*, *mei-1*, *ran-3*, *ima-3*, and *C27D9.1*RNAi were PCR amplified from genomic DNA. Primer sequences were based on the PhenoBank database (http://worm.mpi-cbg.de/phenobank2; Sonnichsen *et al.*, 2005).

Separation of individual chromosomes from *C. elegans* embryos

Condensed chromosomes were separated individually with slight modifications of standard procedures (Albertson and Thomson, 1982; Yoshida *et al.*, 1984). Slides were coated with 1% poly-L-lysine (P9820; Sigma-Aldrich, St. Louis, MO) in distilled water. Distilled water (3 µl) was pipetted onto the slide, and several gravid hermaphrodites (wild-type N2 or treated with RNAi) were placed in the drop and cut open with a scalpel to release the embryos. To prevent artifactual contraction of the chromosomes, drugs inducing metaphase arrest (e.g., colchicine and nocodazole) were not used. After removing most of the distilled water, we placed a drop of 50% acetic acid on the underside of an 18 × 18–mm coverslip, and laid this on top of the drop on the slide. The slide was inverted, and gentle pressure was applied to squash the embryos. The slide was placed on dry ice for at least 10 min. The coverslip was removed, and the slide was placed in 100% ethanol for at least 15 min and then in methanol:acetic acid (3:1) for at least 30 min. The fixed slides were air dried and stained with 2 µg/ml 4′,6-diamidino-2-phenylindole (DAPI) solution for 5 min. A coverslip was placed on the sample and sealed. The sample was visualized at room temperature with an LSM5 LIVE confocal laser-scanning microscope equipped with an oil-immersed plan Apochromat 63× objective of numerical aperture (NA) 1.4 (Carl Zeiss, Jena, Germany) or an FV1000 confocal microscope equipped with an oil-immersed plan Apochromat 100× objective of NA 1.4 (Olympus, Tokyo, Japan).

Nucleus and chromosome assembly in *X. laevis* egg extracts

X. laevis eggs and CSF extracts were prepared as described (Iwabuchi *et al.*, 2000). To reconstruct interphase nuclei, CSF extracts were supplemented with demembranated sperm nuclei (750–1000 nuclei/µl final concentration; Ohsumi *et al.*, 1993), energy solution (1 mM ATP, 10 mM creatine phosphate, and 1 mM $MgCl_2$; Murray, 1991), 5 µM Cy3-dUTP (GE Healthcare, Piscataway, NJ; to visualize DNA replication), and 100 µg/ml cycloheximide (Sigma-Aldrich; to inhibit spontaneous transition to mitosis). All incubations were performed at 22°C unless otherwise stated. After 15 min of incubation, $CaCl_2$ in extraction buffer (EB: 100 mM KCl, 5 mM $MgCl_2$, 20 mM 4-(2-hydroxyethyl)-1-piperazineethanesulfonic acid [HEPES]–KOH, pH 7.5) was added to a final concentration of 0.6 mM to release the extract into interphase, allowing nuclear formation and DNA replication. To inhibit nuclear growth, 200 µg/ml WGA (Wako Pure Chemical Industries, Osaka, Japan) or 0.5 mg/ml anti–lamin LIII antibody (Hasebe *et al.*, 2011) was added after verifying assembly of round nuclei surrounded by the membrane structure. The duration of this preincubation was 30–40 min. In the control experiment, we added 0.5 mg/ml rabbit immunoglobulin G instead of the anti–lamin LIII antibody or 50 µg/ml aphidicolin (Sigma-Aldrich) to inhibit DNA replication. After 90-min incubation (total 120 min after adding sperm nuclei) at 22°C, the mixture was supplemented with a nondestructible cyclin B (60 nM; Iwabuchi *et al.*, 2002) to induce mitosis and incubated for another 60 min. Metaphase spindles with aligned replicated chromosomes generally formed after 60 min.

Observation of reconstructed nuclei and individual chromosomes

To observe reconstructed nuclei in the egg extract, 2 µl of extract containing the interphase nuclei was fixed and stained with 4% formaldehyde in 30% glycerol in EB containing 5 µg/ml Hoechst 33342 and 20 µg/ml 3,3′-dihexyloxacarbocyanine iodide (DiOC6(3); Kodak, Rochester, NY) on the glass slide and observed under a microscope (Nikon Eclipse 80i). To observe individual chromosomes in the *X. laevis* egg extract, extracts containing mitotic spindles were fixed and stained as described, with slight modifications (Funabiki and Murray, 2000). Briefly, 10 µl of egg extract containing condensed chromosomes was mixed with 40 µl of chromosome dilution buffer

(10 mM K-HEPES, pH 7.6, 200 mM KCl, 0.5 mM $MgCl_2$, 0.5 mM ethylene glycol tetraacetic acid [EGTA], and 250 mM sucrose). After 15 min at room temperature, 400 µl of fix solution (4% formaldehyde, 0.1% Triton X-100, 10 mM HEPES-KOH, pH 7.5, 100 mM KCl, 2 mM $MgCl_2$, 0.1 mM $CaCl_2$, and 5 mM EGTA) was added to the diluted chromosomes. After 15 min at room temperature, the fixed chromosome fractions were sedimented onto a poly-L-lysine–coated coverslip through a 1-ml cushion (30% glycerol, 10 mM HEPES-KOH, pH 7.5, 100 mM KCl, 2 mM $MgCl_2$, 0.1 mM $CaCl_2$, and 5 mM EGTA) at 2500 × *g* for 15 min at 4°C. The coverslips were stained with 1 µg/ml Hoechst 33342 and observed by FV1000 confocal microscopy with a 100× objective.

Quantification of chromosome and nuclear sizes

To quantify chromosome lengths in *C. elegans* and *X. laevis*, we manually measured the length of a segmented line traced along DAPI- or Hoechst-positive chromosomes using ImageJ software (National Institutes of Health, Bethesda, MD). For chromosome widths, lines were drawn perpendicular to the path of sister chromatids (avoiding centromeric regions). To measure nuclear size in *C. elegans*, embryos expressing GFP-histone in M9 solution were visualized, and several *z*-sections at 2-µm steps were acquired every 30 s (Hara and Kimura, 2009). The maximum diameter of the nuclei in *C. elegans* embryos and *X. laevis* egg extract was measured using ImageJ.

Chromosome condensation dynamics in *C. elegans* embryos

Chromosome condensation dynamics was characterized as described previously (Maddox *et al.*, 2006). We acquired *z*-sections of GFP–histone-H2B–positive nuclei at 2-µm steps and 10-s intervals from the end of the previous cell division to spindle formation. A maximum intensity projection was selected for each time point. We cut the largest square region that fit within the nucleus for further analysis and set the minimum pixel intensity in each image to 0 and the maximum to 255. After we summed five intensity distributions from 20 s before the target time point to 20 s later, we calculated the percentage of pixels with below-threshold intensity (40%) per total pixels. This threshold (40% = 102) reveals a progressive change in the shape of the fluorescence intensity distribution in one-cell-stage embryos and *smc-4* (RNAi) embryos (Portier *et al.*, 2007). For comparison, we examined these data in different developmental stages.

ACKNOWLEDGMENTS

We thank Tatsuya Hirano and Keishi Shintomi (RIKEN Advanced Science Institute, Wako, Japan) for helping us with visualization of chromosomes and for discussion; Masato T. Kanemaki (National Institute of Genetics, Mishima, Japan) for valuable suggestions; Jon Audhya (University of Wisconsin, Madison, WI) for the *C. elegans* strains; Tomo Kondo (National Institute of Genetics) for technical assistance; Christoph Merten (European Molecular Biology Laboratory, Heidelberg, Germany) for support; and the members of the Cell Architecture Laboratory for helpful discussions. Y.H. was a Research Fellow of the Japan Society for the Promotion of Science. This study was supported by grants from the Ministry of Education, Culture, Sports, Science, and Technology, Japan, and by The Graduate University for Advanced Studies (Sokendai).

REFERENCES

Albertson DG, Thomson JN (1982). The kinetochores of *Caenorhabditis elegans*. Chromosoma 86, 409–428.

Belmont AS, Sedat JW, Agard DA (1987). A three-dimensional approach to mitotic chromosome structure: evidence for a complex hierarchical organization. J Cell Biol 105, 77–92.

Berardino MAD (1962). The karyotype of *Rana pipiens* and investigation of its stability during embryonic differentiation. Dev Biol 5, 101–126.

Briggs R (1949). The influence of egg volume on the development of haploid and diploid embryos of the frog, *Rana pipiens*. J Exp Zool 111, 255–294.

Buongiorno-Nardelli M, Micheli G, Carri MT, Marilley M (1982). A relationship between replicon size and supercoiled loop domains in the eukaryotic genome. Nature 298, 100–102.

C. elegans Sequencing Consortium (1998). Genome sequence of the nematode *C. elegans*: a platform for investigating biology. Science 282, 2012–2018.

Carvalho A, Desai A, Oegema K (2009). Structural memory in the contractile ring makes the duration of cytokinesis independent of cell size. Cell 137, 926–937.

Conklin EG (1912). Cell size and nuclear size. J Exp Zool 12, 1–98.

Courbet S, Gay S, Arnoult N, Wronka G, Anglana M, Brison O, Debatisse M (2008). Replication fork movement sets chromatin loop size and origin choice in mammalian cells. Nature 455, 557–560.

Cox LS (1992). DNA replication in cell-free extracts from *Xenopus* eggs is prevented by disrupting nuclear envelope function. J Cell Sci 101, 43–53.

Cremer T, Cremer C (2001). Chromosome territories, nuclear architecture and gene regulation in mammalian cells. Nat Rev Genet 2, 292–301.

D'Angelo MA, Anderson DJ, Richard E, Hetzer MW (2006). Nuclear pores form de novo from both sides of the nuclear envelope. Science 312, 440–443.

Desai A, Deacon HW, Walczak CE, Mitchison TJ (1997). A method that allows the assembly of kinetochore components onto chromosomes condensed in clarified *Xenopus* egg extracts. Proc Natl Acad Sci USA 94, 12378–12383.

Finlay DR, Meier E, Bradley P, Horecka J, Forbes DJ (1991). A complex of nuclear pore proteins required for pore function. J Cell Biol 114, 169–183.

Frankhauser G (1934). Cytological studies on egg fragments of the salamander *Triton*. V. Chromosome number and chromosome individuality in the cleavage mitoses of merogonic fragments. J Exp Zool 68, 1–57.

Freedman BS, Heald R (2010). Functional comparison of H1 histones in *Xenopus* reveals isoform-specific regulation by Cdk1 and RanGTP. Curr Biol 20, 1048–1052.

Funabiki H, Murray AW (2000). The *Xenopus* chromokinesin Xkid is essential for metaphase chromosome alignment and must be degraded to allow anaphase chromosome movement. Cell 102, 411–424.

Goehring NW, Hyman AA (2012). Organelle growth control through limiting pools of cytoplasmic components. Curr Biol 22, R330–R339.

Greenan G, Brangwynne CP, Jaensch S, Gharakhani J, Julicher F, Hyman AA (2010). Centrosome size sets mitotic spindle length in *Caenorhabditis elegans* embryos. Curr Biol 20, 353–358.

Hachet V, Kocher T, Wilm M, Mattaj IW (2004). Importin alpha associates with membranes and participates in nuclear envelope assembly in vitro. EMBO J 23, 1526–1535.

Hancock R (2012). Structure of metaphase chromosomes: a role for effects of macromolecular crowding. PLoS One 7, e36045.

Hara Y, Kimura A (2009). Cell-size-dependent spindle elongation in the *Caenorhabditis elegans* early embryo. Curr Biol 19, 1549–1554.

Hara Y, Kimura A (2011). Cell-size-dependent control of organelle sizes during development. Results Probl Cell Differ 53, 93–108.

Hara Y, Kimura A (2013). An allometric relationship between mitotic spindle width, spindle length, and ploidy in *Caenorhabditis elegans* embryos. Mol Biol Cell 24, 1411–1419.

Hasebe T, Kajita M, Iwabuchi M, Ohsumi K, Ishizuya-Oka A (2011). Thyroid hormone-regulated expression of nuclear lamins correlates with dedifferentiation of intestinal epithelial cells during *Xenopus laevis* metamorphosis. Dev Genes Evol 221, 199–208.

Hirano T, Mitchison TJ (1994). A heterodimeric coiled-coil protein required for mitotic chromosome condensation in vitro. Cell 79, 449–458.

Hirano T, Kobayashi R, Hirano M (1997). Condensins, chromosome condensation protein complexes containing XCAP-C, XCAP-E and a *Xenopus* homolog of the *Drosophila* Barren protein. Cell 89, 511–521.

Hudson DF, Vagnarelli P, Gassmann R, Earnshaw WC (2003). Condensin is required for nonhistone protein assembly and structural integrity of vertebrate mitotic chromosomes. Dev Cell 5, 323–336.

Ishii K, Arib G, Lin C, Van Houwe G, Laemmli UK (2002). Chromatin boundaries in budding yeast: the nuclear pore connection. Cell 109, 551–562.

Iwabuchi M, Ohsumi K, Yamamoto TM, Kishimoto T (2002). Coordinated regulation of M phase exit and S phase entry by the Cdc2 activity level in the early embryonic cell cycle. Dev Biol 243, 34–43.

Iwabuchi M, Ohsumi K, Yamamoto TM, Sawada W, Kishimoto T (2000). Residual Cdc2 activity remaining at meiosis I exit is essential for meiotic M-M transition in *Xenopus* oocyte extracts. EMBO J 19, 4513–4523.
Jallepalli PV, Lengauer C (2001). Chromosome segregation and cancer: cutting through the mystery. Nat Rev Cancer 1, 109–117.
Kieserman EK, Heald R (2011). Mitotic chromosome size scaling in *Xenopus*. Cell Cycle 10, 3863–3870.
Kimura A, Onami S (2005). Computer simulations and image processing reveal length-dependent pulling force as the primary mechanism for *C. elegans* male pronuclear migration. Dev Cell 8, 765–775.
Ladouceur AM, Ranjan R, Maddox PS (2011). Cell size: chromosomes get slapped by a midzone ruler. Curr Biol 21, R388–R390.
Levy DL, Heald R (2010). Nuclear size is regulated by importin alpha and Ntf2 in *Xenopus*. Cell 143, 288–298.
Levy DL, Heald R (2012). Mechanisms of intracellular scaling. Annu Rev Cell Dev Biol 28, 113–135.
Lourim D, Kempf A, Krohne G (1996). Characterization and quantitation of three B-type lamins in *Xenopus* oocytes and eggs: increase of lamin LI protein synthesis during meiotic maturation. J Cell Sci 109, 1775–1785.
Maddox PS, Portier N, Desai A, Oegema K (2006). Molecular analysis of mitotic chromosome condensation using a quantitative time-resolved fluorescence microscopy assay. Proc Natl Acad Sci USA 103, 15097–15102.
Mains PE, Kemphues KJ, Sprunger SA, Sulston IA, Wood WB (1990). Mutations affecting the meiotic and mitotic divisions of the early *Caenorhabditis elegans* embryo. Genetics 126, 593–605.
Maresca TJ, Freedman BS, Heald R (2005). Histone H1 is essential for mitotic chromosome architecture and segregation in *Xenopus laevis* egg extracts. J Cell Biol 169, 859–869.
Meyerzon M, Gao Z, Liu J, Wu JC, Malone CJ, Starr DA (2009). Centrosome attachment to the *C. elegans* male pronucleus is dependent on the surface area of the nuclear envelope. Dev Biol 327, 433–446.
Micheli G, Luzzatto AR, Carri MT, de Capoa A, Pelliccia F (1993). Chromosome length and DNA loop size during early embryonic development of *Xenopus laevis*. Chromosoma 102, 478–483.
Murray AW (1991). Cell cycle extracts. Methods Cell Biol 36, 581–605.
Nasmyth K (2002). Segregating sister genomes: the molecular biology of chromosome separation. Science 297, 559–565.
Neurohr G, Naegeli A, Titos I, Theler D, Greber B, Diez J, Gabaldon T, Mendoza M, Barral Y (2011). A midzone-based ruler adjusts chromosome compaction to anaphase spindle length. Science 332, 465–468.
Ohsumi K, Katagiri C, Kishimoto T (1993). Chromosome condensation in *Xenopus* mitotic extracts without histone H1. Science 262, 2033–2035.
Ono T, Losada A, Hirano M, Myers MP, Neuwald AF, Hirano T (2003). Differential contributions of condensin I and condensin II to mitotic chromosome architecture in vertebrate cells. Cell 115, 109–121.
Pflumm MF (2002). The role of DNA replication in chromosome condensation. Bioessays 24, 411–418.
Portier N, Audhya A, Maddox PS, Green RA, Dammermann A, Desai A, Oegema K (2007). A microtubule-independent role for centrosomes and aurora a in nuclear envelope breakdown. Dev Cell 12, 515–529.
Poteryaev D, Squirrell JM, Campbell JM, White JG, Spang A (2005). Involvement of the actin cytoskeleton and homotypic membrane fusion in ER dynamics in *Caenorhabditis elegans*. Mol Biol Cell 16, 2139–2153.
Segbert C, Barkus R, Powers J, Strome S, Saxton WM, Bossinger O (2003). KLP-18, a Klp2 kinesin, is required for assembly of acentrosomal meiotic spindles in *Caenorhabditis elegans*. Mol Biol Cell 14, 4458–4469.
Seydoux G, Dunn MA (1997). Transcriptionally repressed germ cells lack a subpopulation of phosphorylated RNA polymerase II in early embryos of *Caenorhabditis elegans* and *Drosophila melanogaster*. Development 124, 2191–2201.
Shintomi K, Hirano T (2011). The relative ratio of condensin I to II determines chromosome shapes. Genes Dev 25, 1464–1469.
Sonnichsen B *et al*. (2005). Full-genome RNAi profiling of early embryogenesis in *Caenorhabditis elegans*. Nature 434, 462–469.
Yoshida TH, Sadaie T, Sadaie Y (1984). Somatic and meiotic chromosomes of the small free-living nematode, *Caenorhabditis elegans*. Proc Jpn Acad B 60, 54–57.